COLOR CODING FOR PARTICLE IAMGE VELOCIMETRY

A.A. SAVIN

Departament of Radio Engineering Fundamentals, National Research University "Moscow Power Engineering Institute", Moscow, 111250, Russia

Corresponding author: Tel.: +79167323279; Fax: +79167323279; Email: alekseisavin@yandex.ru

KEYWORDS:
Main subjects: flow visualization
Fluid: high speed flows
Visualization method(s): particle image velocimetry
Other keywords: image processing, color coding

INTRODUCTION: As it's known [1], at correlation analysis of flow visualization images are possible two variants. In the first two-pulse laser illumination of a flow is used the image of particles collects on one frame. In this case the received image consists of set of paires particles and by means of calculation of autocorrelation function (ACF) their shift in time between two impulses of illumination is defined. The second variant consists in record separately two consecutive divided image of a flow and further cross-correlation function (CCF) is calculated. If instead of two to use more quantity of the images for the analysis there is a possibility to operate the form of correlation functions by means of coding.

CODING In RADIO ENGINEERING: To begin with it is necessary to tell, about what coding meaning in this report. This problem has appeared in radio engineering in connection with detection of a signal against noise. For example, it could be seen at radiolocation scanning of other planets of solar system. It is easily possible to imagine, with what noise was returned the signal. There is a theory of optimum detection of signals [2] according to which the greatest signal-to-noise ratio can be reached on an exit of the so-called optimum filter. The signal form on exit of such filter will match with autocorrelation function of an entrance signal, to within time shift. In this connection there was a question on at what signals the form of autocorrelation function will be the most suitable to extraction of a signal from noise. For this purpose it is necessary mass energy of a signal to direct in the main peak ACF, whenever possible having suppressed thus all other peaks to avoid false detection of a signal. Use as a signal sequence of impulses with voltages different in a sign - codes became one of candidates solution of the yielded problem.

The most optimum code from the point of view of the above-stated requirements to ACF, are Barker's codes [2]. They are remarkable that at length of a code in N symbols sidelobes have the fixed level, in N time smaller, than level of the main peak of autocorrelation function. The example of a 13-item Barker's code is shown in Fig 1. The basic problem with Barker's codes is that for length of a code is more than 13 symbols such codes do not exist. Therefore the big widespread was received by so-called pseudo-random sequences of the maximum length or M-sequence. At them level of sidelobes different, but all of them at length of code N do not exceed value $1/\sqrt{N}$. The example of a 15-item M-sequence it is shown in Fig 1.

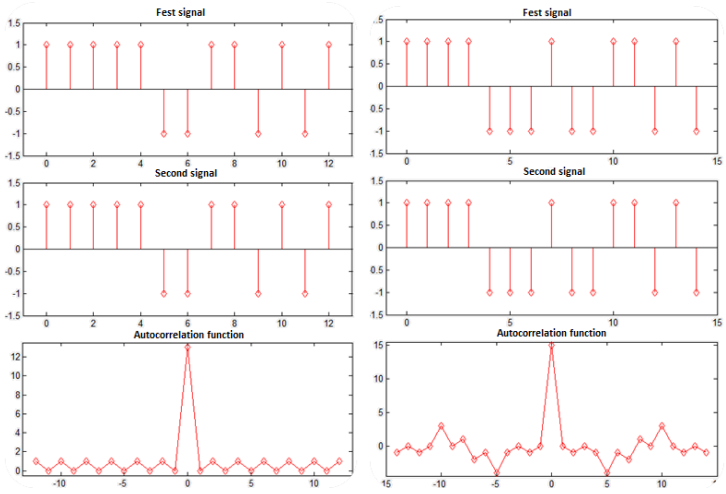

Fig. 1 Autocorrelation functions for a 13-item Barker's code (at the left) and 15-item M-sequence (on the right)

COLOR CODING Of ACF: To apply idea of coding to the flow visualization images, two lasers, red and green, the color video camera with the analog-to-digital converter, a control unit for lasers and PC is required. After transformation of the image to the digital form the received array can be divided, under certain conditions, on two components, red and green. If to make inversion on a sign, for example, a green component of the image, and then to combine two arrays in one the trace of each particle will represent sequence of various impulses on a sign, that is a code. Selection sequence of illumination impulses it is possible to receive the different codes more convenient for calculation of a flow's vector field. The example of such approach is shown in Fig 2.

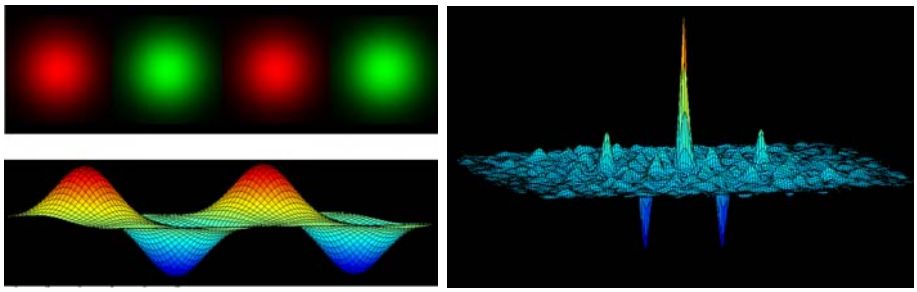

Fig. 2 Trace of a particle (at the left from above), the respective coded signal (at the left from below) and autocorrelation function of the coded signal (on the right)

From autocorrelation function for a four-pulse signal with a color code {red, green, red, green}, shown in Fig 2, it is clear that the first side peaks on which displacement is defined, are pronounced and in area of negative values of function that facilitates a problem of their separation.

For comparison accuracy characteristics of a classical two-frame PIV-method and a color four-pulse PIV-method the following model of the PIV-image was used:

- A format of image N_x by N_y pixels;
- Each particle represents two-dimensional Gauss curve [3]; the size of a particle is at the mean five pixels plus the random deviation chosen under the Gauss law with zero meaning value and dispersion is one; brightness of each particle chosen under the uniform law from 125 to 255; number of particles N_p; coordinates of particles on the first image chosen also under the uniform law from 1 to N_x on coordinate x, and from 1 to N_y on coordinate y; on the subsequent images coordinate of particles were received by uniform shifting;
- To the images normal noise with a zero meaning value and a various dispersion (σ^2) was added.

The received images was processioned with following algorithms.

Algorithm of a classical two-frame PIV-method.

The black-and-white digital image is represented in the arrow of the dimension N_x by N_y, where N_x by N_y - the size of the camera's CCD matrix. We will indicate the image, as $I(i, j)$, where $1 \le i \le N_x$, $1 \le j \le N_y$. The size of investigation area (a_I) is N_{ai} by N_{ai} pixels. Interrogation area is shifted on d pixels.

Images were processioned on following algorithm.

1. Splitting of the image into interrogation areas (further actions are carried out for each area of interest).

2. Search CCF (R_{II}) between interrogation area on the first image (a_{I1}) and dilated on $N_{ai}/2$ pixels from each side of interrogation area of the second image (a_{I2}, if it necessary, interrogation area on the second image is complemented with zero):

$$R_{II}\left(m,n\right) = \sum_{i=-N_{ai}/2}^{3N_{ai}/2} \sum_{j=-N_{ai}/2}^{3N_{ai}/2} a_{I1}\left(i,j\right) \cdot a_{I2}\left(i+m, j+n\right). \quad (1)$$

3. Definition CCF's coordinates of maximum with accurate within pixel (d_x - coordinate x, d_y - coordinate y):

$$\begin{aligned} d_x &= \max\left(R_{II}\left(m,n\right)\right)_m, \\ d_y &= \max\left(R_{II}\left(m,n\right)\right)_n. \end{aligned} \quad (2)$$

4. Definition CCF's coordinates of maximum with accurate within subpixel by means of three-point match of the curve of Gauss (Δ_x - coordinate x, Δ_y - coordinate y) [3]:

$$\begin{aligned} \Delta_x &= \frac{\ln\left(R_{II}\left(d_x-1,d_y\right)\right) - \ln\left(R_{II}\left(d_x+1,d_y\right)\right)}{2\cdot\ln\left(R_{II}\left(d_x-1,d_y\right)\right) - 4\cdot\ln\left(R_{II}\left(d_x,d_y\right)\right) + 2\cdot\ln\left(R_{II}\left(d_x+1,d_y\right)\right)}, \\ \Delta_y &= \frac{\ln\left(R_{II}\left(d_x,d_y-1\right)\right) - \ln\left(R_{II}\left(d_x,d_y+1\right)\right)}{2\cdot\ln\left(R_{II}\left(d_x,d_y-1\right)\right) - 4\cdot\ln\left(R_{II}\left(d_x,d_y\right)\right) + 2\cdot\ln\left(R_{II}\left(d_x,d_y+1\right)\right)}. \end{aligned} \quad (3)$$

As a result coordinate of the maximum, equal to projections of displacement vectors (s_x - coordinate x, s_y - coordinate y):

$$\begin{aligned} s_x &= d_x + \Delta_x, \\ s_y &= d_y + \Delta_y. \end{aligned} \quad (4)$$

5. The magnitude of a displacement vector in a fragment is defined:

$$D_m = \sqrt{\left(s_x\right)^2 + \left(s_y\right)^2}. \quad (5)$$

6. Output of a vector field of speeds.

Algorithm of processing of the PIV-image with color coding of ACF.

The color digital image is represented in the array of the dimension N_x by N_y by 3, where N_x by N_y - the size camera's CCD matrix. The third dimension defines color in RGB format. So, we will indicate the image, as $I(i, j, k)$, where $1 \le i \le N_x$, $1 \le j \le N_y$, $1 \le k \le 3$. The size of interrogation area (a_I) iss N_{ai} by N_{ai} pixels. Interrogation area is shifted on d pixels.

Image was processioned on following algorithm.

1. Splitting of the image into interrogation areas (further actions are carried out for each interrogation area):

2. Inversion of a green component of a fragment (x, y - coordinates of current interrogation area):

$$a_I\left(x,y\right) = I\left(x,y,1\right) - I\left(x,y,2\right). \quad (6)$$

3. Search of autocorrelation function (R_I) of interrogation areas:

$$R_I\left(m,n\right) = \sum_{i=1}^{N_{ai}} \sum_{j=1}^{N_{ai}} a_I\left(i,j\right) \cdot a_I\left(i+m, j+n\right). \quad (7)$$

4. Definition ACF's maximum coordinates with accurate within pixel (d_x - coordinate x, d_y - coordinate y):

$$\begin{aligned} d_x &= \max\left(R_I\left(m,n\right)\right)_m, \\ d_y &= \max\left(R_I\left(m,n\right)\right)_n. \end{aligned} \quad (8)$$

5. Definition ACF's maximum coordinates with accurate within subpixel by means of three-point match of the curve of Gauss (Δ_x - coordinate x, Δ_y - coordinate y):

$$\begin{aligned} \Delta_x &= \frac{\ln\left(R_I\left(d_x-1,d_y\right)\right)-\ln\left(R_I\left(d_x+1,d_y\right)\right)}{2\cdot\ln\left(R_I\left(d_x-1,d_y\right)\right)-4\cdot\ln\left(R_I\left(d_x,d_y\right)\right)+2\cdot\ln\left(R_I\left(d_x+1,d_y\right)\right)}, \\ \Delta_y &= \frac{\ln\left(R_I\left(d_x,d_y-1\right)\right)-\ln\left(R_I\left(d_x,d_y+1\right)\right)}{2\cdot\ln\left(R_I\left(d_x,d_y-1\right)\right)-4\cdot\ln\left(R_I\left(d_x,d_y\right)\right)+2\cdot\ln\left(R_I\left(d_x,d_y+1\right)\right)}. \end{aligned} \quad (9)$$

As a result coordinate of maximum (D_x - coordinate x, D_y - coordinate y):

$$\begin{aligned} D_x &= d_x+\Delta_x, \\ D_y &= d_y+\Delta_y. \end{aligned} \quad (10)$$

6. Similarly under equations (8)-(10) coordinates of side ACF's maximum ($D_{\pm x}$, $D_{\pm y}$) are defined. For this purpose ACF is necessary to invert at first:

$$\overline{R_I}\left(m,n\right)=-R_I\left(m,n\right). \quad (11)$$

7. The magnitude of displacement vector in a fragment is defined:

$$D_m=\sqrt{\left(D_x-D_{\pm x}\right)^2+\left(D_y-D_{\pm y}\right)^2}. \quad (12)$$

8. Direction definition by CCF (R_{II}) between red (a_{Ir}):

$$a_{Ir}\left(x,y\right)=I\left(x,y,1\right),$$

and green (a_{Ig}):

$$a_{Ig}\left(x,y\right)=I\left(x,y,2\right)$$

fragment components:

$$R_{II}\left(m,n\right)=\sum_{i=1}^{N_{ai}}\sum_{j=1}^{N_{ai}}a_{Ir}\left(i,j\right)\cdot a_{Ig}\left(i+m,j+n\right). \quad (13)$$

For R_{II} under the equation (8) there are integer coordinates of a maximum (d_{IIx}, d_{IIy}) and projections of vectors (s_x, s_y) are received:

$$\begin{aligned} s_x &= sign(d_{IIx}-d_x)\left|D_x-D_{\pm x}\right|, \\ s_y &= sign(d_{IIy}-d_y)\left|D_y-D_{\pm y}\right|. \end{aligned} \quad (14)$$

In (14) function *sing (x)* gives an argument sign.

9. Output of a vector field of speeds.

The algorithm of modeling of the PIV-image described above has been applied at following installations of model:

$N_x = N_y = 1024$ pixels;

$N_p = 15000$ particles.

The dispersion of noise (σ^2) variated from 0.01 to 0.1 with step 0.01 (a dispersion normalized to a square of voltage of a signal).

Parameters of processing algorithm of the PIV-image with color coding:

N_{ai} = 40 pixels;

d = 20 pixels.

At the yielded parameters from each image 2500 vectors are received. For each dispersion of noise total number of the measured vectors N = 7500 was analyzed three plotting, hence.

By results of processing the array of the measured magnitude of displacement vectors (D_m) for each signal-to-noise ratio is received. By results of these measurements the meaning value (m) was calculated:

$$m = \frac{\sum_{i=1}^{N} \delta D_i}{N}, \quad (15)$$

And root mean square (RMS):

$$RMS = \sqrt{\frac{\sum_{i=1}^{N} \left(\delta D_i - m\right)^2}{N-1}}, \quad (16)$$

Measurement relative error (δD):

$$\delta D = \frac{\left|D_m - D_r\right|}{D_r} \cdot 100\%. \quad (17)$$

The received graph of dependence of a mathematical expectation (m) and RMS of a relative error of measurement from the signal-to-noise ratio (q) for two above described methods are shown in Fig 3. As a noise dispersion normalized to voltage of a signal the signal-to-noise ratio is calculated under the following formula:

$$q = 10 \cdot \lg\left(\frac{1}{\sigma^2}\right).$$

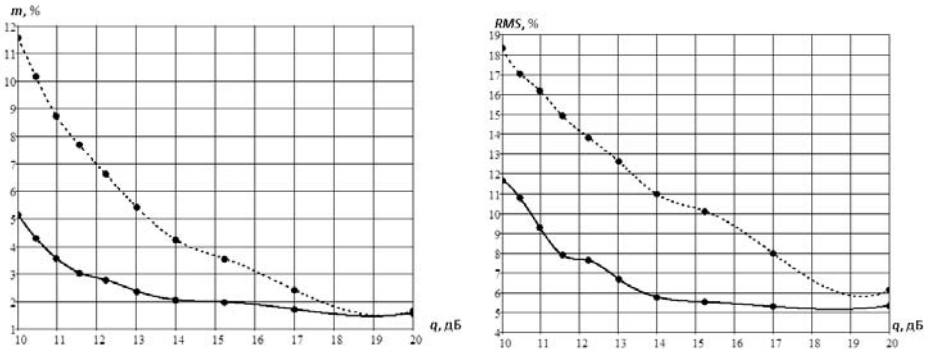

Fig. 3 Mathematical expectation (at the left) and root mean square (on the right) a relative error of measurement for the classical two-frame PIV-analysis (dotted lines) and four-pulse PIV-analysis with color encoding

From Fig 3 it is clear that at small signal-to-noise ratio the four-pulse PIV-method with color coding is more accuracy, and with reduction of the signal-to-noise ratio an advantage in accuracy to become more and more significant. It is possible to explain it to that in this case ACF's maximum have bigger value, than in a classical two-frame mode. Besides, at inversion of a green component of the image there is particulate balancing of noise on red and green components of the image.

At increases of the signal-to-noise ratio both methods show identical accuracy as at small noise the basic contribution to an error makes definition of function's maximum that in both methods becomes under the equation (9).

COLOR CODING Of CCF: The Basic problem of autocorrelation analysis is the impossibility to define a direction of flow. It is necessary to do it by additional means (equations (13)-(14)). Therefore color coding of CCF more attractively. Requirements to form of CCF are simple: it is necessary, that it had a strongly pronounced main maximum, and all side maximum were as it is possible smaller.

At once we will notice that the more long coding sequence, the it is necessary to choose the bigger size of interrogation area and that less obtains the yielded data of a PIV-method. For this cause the coding sequences which length does not exceed five have been considered. Research of these sequences has shown that to achieve the optimum CCF's form, two coding colors it has not enough. Not to add the third laser, the decision to use simultaneous flash of red and green lasers which yields the third color - yellow was accepted. Then the algorithm of color encoding CCF looks as follows.

After the total image is created, there is its division into three components: red, green and yellow (for allocation of a yellow component the pixels of the image having identical value of red and green components) are searched. Then it is created two summary image in which these three color components are summarized with different scales, and are calculated CCF of image fragments. Such approach is shown in Fig 4.

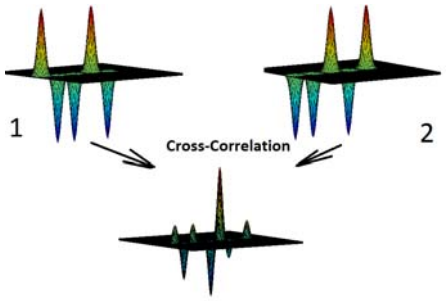

Fig. 1 Coding of cross-correlation functions

Coding sequences for length of a code three, four and five symbols which provide greatest possible for the yielded length of a code level of main CCF's maximum whereas side maximums on the value do not exceed one have been found. For a three-symbolical code it is sequence {red, green, yellow}. In the first and second image to the red value of one, green - one and a minus one accordingly, yellow - a minus one and one accordingly is appropriated. We receive two codes {1, 1,-1} and {1,-1, 1}. For a four-symbolical code color sequence is {red, green, yellow, green} and the appropriate codes are {1, 1,-1, 1} and {1,-1, 1,-1}. For a five-symbolical code color sequence {red, green, yellow, red, yellow} and the appropriate codes {1,-1,-1, 1,-1} and {-1,-1, 1,-1, 1}.

CONCLUSION: Use of color coding in a PIV-method allows to achieve more optimum form of correlation functions from the point of view of peas allocation. Thus results of processing have shown that at small signal-to-noise ratio the multi-pulse PIV-method with color coding yields higher accuracy, than a usual two-frame PIV-method.

Coding of the cross-correlation function is developed for possibility of automatic definition of flow direction and optimum codes for sequences, of three, four and five symbols are founded.

References

1. Raffe M. et al. *Particle Image Velocimetry: A Practical Guide.* Springer, Berlin, 2007
2. Финкельштейн М. И. *Основы Радиолокации.* Радио и Связь, Москва, 1983
3. Marxen M. et al. *Comparison of Gaussian particle center estimators and the achievable measurement density for particle tracking velocimetry.* Experiments in Fluids. 2000, 29, pp. 145-153